

Article

Air Pollution and Mobility, What Carries COVID-19?

C. Vladimir Rodríguez-Caballero ^{1,*}  and J. Eduardo Vera-Valdés ^{2,†} 

¹ Department of Statistics, ITAM, Río Hondo No. 1, Col. Progreso Tizapán, Álvaro Obregón, CDMX, Ciudad de México 01080, Mexico

² Department of Mathematical Sciences, Aalborg University, 9220 Aalborg, Denmark; eduardo@math.aau.dk

* Correspondence: vladimir.rodriguez@itam.mx

† CREATES, 8210 Aarhus, Denmark.

Abstract: This paper tests if air pollution serves as a carrier for SARS-CoV-2 by measuring the effect of daily exposure to air pollution on its spread by panel data models that incorporates a possible commonality between municipalities. We show that the contemporary exposure to particle matter is not the main driver behind the increasing number of cases and deaths in the Mexico City Metropolitan Area. Remarkably, we also find that the cross-dependence between municipalities in the Mexican region is highly correlated to public mobility, which plays the leading role behind the rhythm of contagion. Our findings are particularly revealing given that the Mexico City Metropolitan Area did not experience a decrease in air pollution during COVID-19 induced lockdowns.

Keywords: pandemic; SARS-CoV-2; carrier; mobility



Citation: Rodríguez-Caballero, C. Vladimir, and J. Eduardo Vera-Valdés. 2021. Air Pollution and Mobility, What Carries COVID-19? *Econometrics* 9: 37. <https://doi.org/10.3390/econometrics9040037>

Academic Editor: Kajal Lahiri

Received: 13 August 2021

Accepted: 24 September 2021

Published: 11 October 2021

Publisher's Note: MDPI stays neutral with regard to jurisdictional claims in published maps and institutional affiliations.



Copyright: © 2021 by the authors. Licensee MDPI, Basel, Switzerland. This article is an open access article distributed under the terms and conditions of the Creative Commons Attribution (CC BY) license (<https://creativecommons.org/licenses/by/4.0/>).

1. Introduction

The COVID-19 pandemic is one of the most severe health crises in recent memory. The official death toll worldwide surpassed 4.5 million as of 15 September 2021. Considering reporting problems in some countries, the actual death toll may not be known for several years. In economic terms, Rodríguez-Caballero and Vera-Valdés (2020) recently show that shocks originated by pandemics in recent times such as COVID-19 seem to have a permanent effect on growth and unemployment. Even though the pandemic is still ongoing, much knowledge has been gained in the past few months regarding the effect of air pollution on morbidity. The most prevalent comorbidities seem to be hypertension, diabetes, cardiovascular and respiratory diseases; see Chudasama et al. (2020); Farias Costa et al. (2020); Yang et al. (2020), among others. Furthermore, some evidence has been obtained regarding the effect that air pollution has on morbidity.

At the local level, the evidence seems to point to a positive correlation between long-term air pollution exposure, particularly Particulate Matter (PM), and the death toll due to COVID-19. Refs. (Bianconi et al. 2020; Comunian et al. 2020; Conticini et al. 2020; Frontera et al. 2020; Gupta et al. 2020; López-Feldman et al. 2021; Son et al. 2020; Travaglio et al. 2021; Yao et al. 2020) find a positive correlation between exposure to PM 2.5, inhalable particles with diameters of 2.5 micrometers and smaller, and a higher number of deaths for the United States, Italy, and Asian cities, among other countries. In contrast, Rodríguez-Villamizar et al. (2020) do not find evidence of an association between long-term exposure to PM 2.5 and COVID-19 mortality rate at the municipality level in Colombia, while Vera-Valdés (2021) finds there is no evidence at the macro-level. Moreover, the evidence of the effect of PM 10, inhalable particles with diameters of 10 micrometers and smaller, and SO₂, sulfur dioxide, on the number of deaths is less established.

Furthermore, some authors have analyzed the short-term correlation between air pollution and the number of cases and deaths due to the pandemic (Borisova and Komisarenko 2020; Setti et al. 2020). Previous studies for other viruses and bacteria inspire the hypothesis that air pollution could act as a carrier for the virus (Groulx et al. 2018; Marquès et al. 2021). That is, the air pollution-to-human transmission channel.

Simultaneous reductions in air pollution and mobility due to lockdowns could lead to loss of evidence to support the carrier hypothesis. For instance, [Coccia \(2021\)](#) find that the effect of air pollution on deaths is larger before the lockdowns, while the effect of interpersonal contacts is maintained. The authors use population density as a proxy for interpersonal contacts. A shortcoming of their selected interpersonal contacts factor is that it does not change during the lockdown, making it harder to disentangle the effect of the human-to-human transmission channel.

In this paper, we disentangle the effect that air pollution and mobility restrictions have on the spread of SARS-CoV-2 using daily data on the death toll, the number of cases due to COVID-19, and contaminants (PM10, and PM2.5) for every municipality from the Mexico City Metropolitan Area (MCMA). The particular characteristics of the MCMA in terms of its high level of workers in the informal sector and the high population density make it an interesting test case. In contrast to other regions, air pollution levels in the MCMA did not significantly decrease during the lockdowns, see [Vera-Valdés and Rodríguez-Caballero \(2021\)](#). Thus, the region's specific characteristics allow us to assess the effect that air pollution levels have on the spread of the virus as an exogenous factor from the economic restrictions. In this regard, the MCMA serves as an ideal test case for the carrier hypothesis. To the best of our knowledge, we are the first to test if air pollution serves as a carrier for SARS-CoV2 by controlling for the effect of mobility restrictions.

The complex interaction of the studied phenomenon makes that pure cross-sectional or time-series econometric models are not the best choice to provide comprehensive insights. To achieve our goal, we form a balanced panel data using the variables of the municipalities from the MCMA explained just above. We make use of the Exponent of Cross-sectional Dependence test of [Bailey et al. \(2016\)](#) to investigate the degree of inter-linkages between all variables involved in the study. The literature on cross-sectional dependence distinguishes between weak (e.g., spatial models) and strong (e.g., factor models) types of dependence. After ensuring stationarity, we find that the municipalities' cross-dependence is very strong encouraging the use of common factor structures to avoid inconsistent estimates commonly found in panel models that ignore such cross-sectional dependence.

We employ panel data models whose strong cross-sectional dependence is introduced by unobservable common factors that may have different effects on the number of daily cases or the number of daily death toll across municipalities. Such factors could include, to mention a few, public mobility across municipalities, or climate conditions. The heterogeneous impact of such factors may be consequence of country/municipality-specific economic or mobility restrictions due to the current pandemic, or the own population lifestyle in a region. We estimate the model adopting two different approaches; (i) by the common correlated effects approach proposed by [Pesaran \(2006\)](#), and by the unobservable multiple interactive effects approach of [Bai \(2009\)](#), see [Westerlund and Urbain \(2015\)](#) for an analytical comparison between both approaches.

Our findings indicate that contemporaneous exposure to pollutants is not statistically significant in explaining the virus's spread once we account for cross-sectional dependence between municipalities. Moreover, we show that this unobservable common factor is highly correlated to public mobility, measured using data from the COVID-19 community mobility reports collected by [Google \(2020\)](#). Consequently, we argue that contemporaneous exposure to pollutants is not the main driver behind the number of cases and deaths due to COVID-19 in the short-term, but the public mobility.

Our results also provide a clear explanation behind the non-significant contemporaneous effects find, inter alia, by [López-Feldman et al. \(2021\)](#), who use a microeconomic approach to show that long-term air pollution exposure (through PM2.5) increases the probability of death due to COVID-19 in the MCMA, particularly for the elderly.

Overall, joining results from literature focused on the long-term and that of this paper with emphasis on the short-term, policymakers will find two relevant warnings.

First, long-term exposure to air pollutants is associated with a higher COVID-19 death toll. Thus, pollution-reducing policies can lessen health risks in the long term.

Second, this pandemic has shown that the worst scenarios are emerging in areas commonly associated with high population density and a highly dynamic lifestyle. Henceforth, to help control the death toll due to COVID-19, we invite governments to implement policies to reduce mobility during the pandemic. Since mobility constraints are the main driver behind the pace of contagion, it can help in reducing the number of deaths due to COVID-19 in the short term.

The rest of the paper is organized as follows: Section 2 describes the geographic region where the MCMA is located, the complex dynamic lifestyle of the city, the government restriction due to COVID 19, and the data used in the study. Section 3 explains the econometric methodology employed in the paper. In Section 4, stationarity and the type of dependence of data is investigated, while Section 5 presents the main results of the effect that air pollution and mobility restrictions have on the spread of SARS-CoV-2. Section 6 discusses some possible extensions and limitations of the study. Finally, Section 7 concludes.

2. The Mexico City Metropolitan Area

Mexico City is the capital and largest city of Mexico. The fastest growth rate in the city occurred in the middle of the last century due to industrialization that caused large rural to urban migrations. Furthermore, population migrations impacted the growth of some satellite towns in the east and the north of the city. Nowadays, these sectors are still the most crowded zones of the MCMA; see Figure 1.

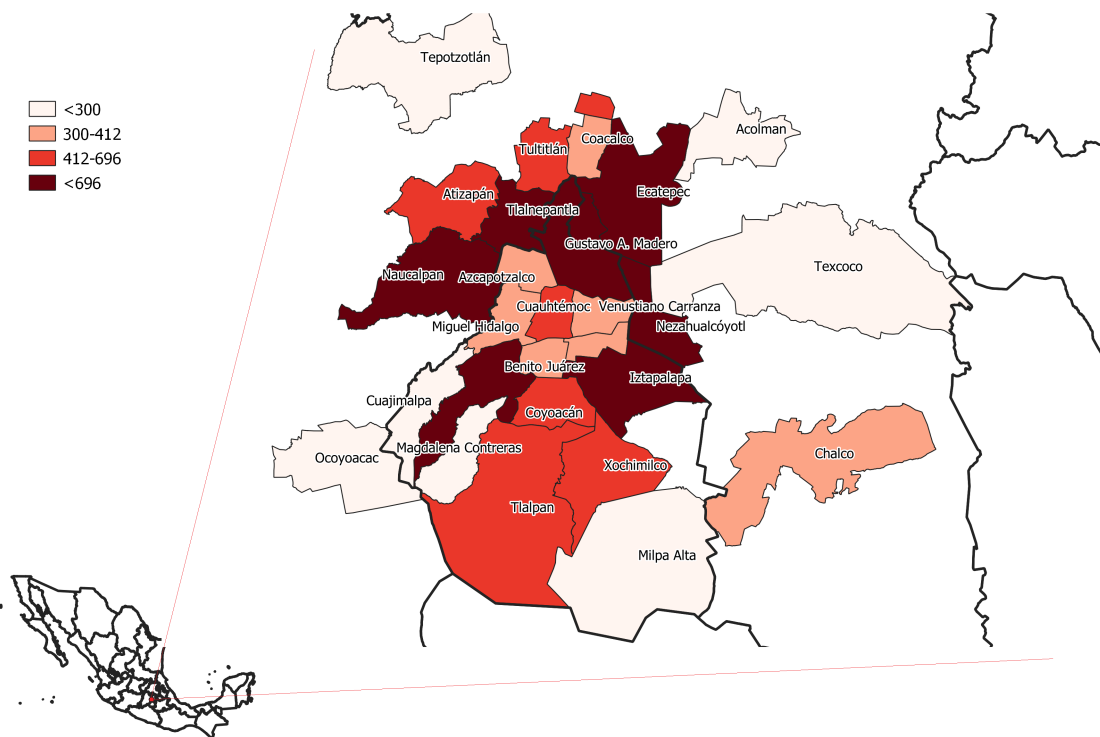


Figure 1. MCMA's population (in thousands) in 2019. Source: Compiled by the authors using official data from state, municipal, and locality boundary files from the Mexican National Institute of Statistics, Geography and Informatics (INEGI).

The metropolitan-wide transport network is mainly composed of a system of 12 subways lines, six bus-rapid-transit (BRT) corridors, and another peripheral BRT system that cover some municipalities in the border of the MCMA. Most of the recent transport lines have connected the areas of higher population density aforementioned with the financial and business districts of the city, which are mostly located in the center (Benito Juárez, Cuauhtémoc, and Miguel Hidalgo municipalities). Figure A1 in Appendix A shows the daily mobility from the most populous periphery towards the city center in 2019. As

seen, there is a decrease in the intensity of the mobility in these public transports on weekends, showing that during non-working days, the financial and business districts are less crowded.

Air quality is one of the MCMA's biggest problems. Located in a valley surrounded by mountains and an average altitude of 2200 meters above sea level, the city's topography does not help to disperse pollution. Air pollution is generated by a wide range of economic activities. However, the city's local government has concentrated its efforts to reduce contaminants generated by the dense daily traffic of one of the heaviest congested cities in the world according to the TomTom Traffic Index¹. Consequently, air pollution is frequently trapped above the city, allowing pollutants to accumulate given the basin's limited ventilation.

The highest concentration of pollutants is frequently observed in the city's industrial northern section; see Figure 2. Even if it is a bit challenging to attribute the sources of pollutants, several authors point out that the high concentrations of some contaminant particles in the northern MCMA are a consequence of industrial processes and waste incinerators in the northern part of the city (Moffet et al. 2008; Molina and Molina 2002). Furthermore, Guerra (2015) finds that municipalities with a higher proportion of households with one or more cars are located in the south and western sections of the city, which shows that there is a low correlation between municipalities with the highest proportion of households with cars and the most polluting regions of the city.

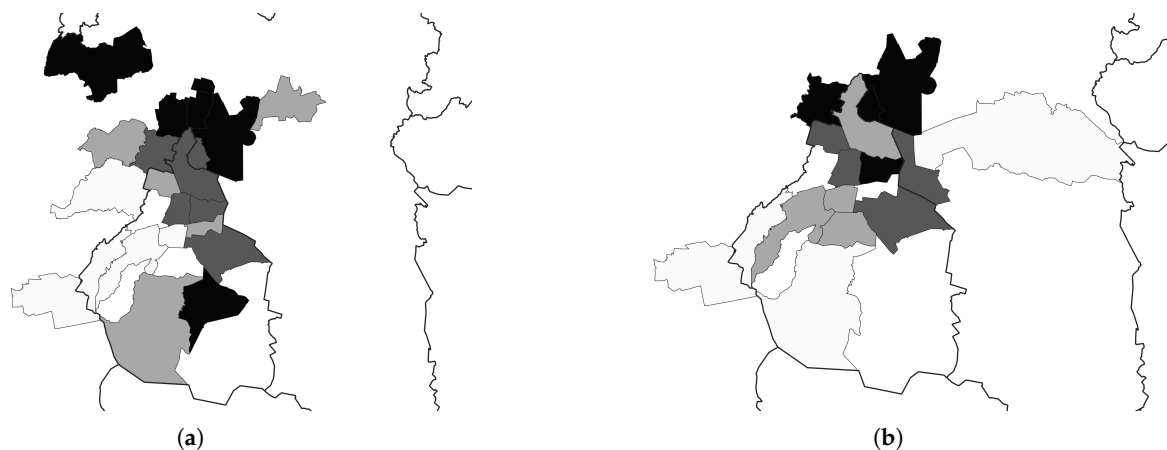


Figure 2. Plots of annual average of contaminants PM10 (panel a), and PM2.5 (panel b) in ppb in the MCMA in 2019. In each panel, the darker the region, the more polluted it is. Source: Compiled by authors using data by Mexico City's Automatic Air Quality Monitoring Network (RAMA).

2.1. Data

The data for this analysis come from Mexico City's data repository². We gathered data on PM 10 and PM 2.5 levels at all stations, and the number of cases and deaths due to COVID-19 for every municipality. The data cover the pandemic's first wave from 12 January 2020, to 31 July 2020.

Furthermore, we collected daily data on mobility from the COVID-19 community mobility reports collected by Google (2020). The reports were based on anonymous data from people who opted-in to storing their location history. For context, 74.7% of the population had access to smartphones, and Android is the operating system in 91% of smartphones sold in the country; see Instituto Federal de Telecomunicaciones (2020). Thus, the data are reliable for detecting public mobility variations.

Each report contains information about mobility in six categories: retail and recreation, grocery and pharmacy, parks, transit stations, workplaces, and residences. The data cover several months and reports percentage changes in mobility from a baseline day representing a typical value for that day of the week. The baseline day is the median value from the 5-week period 3 January to 6 February 2020. In the analysis, we focus on the first four mobility indexes described above, given the high level of weekly seasonality for the index on workplaces and the negative relation of the residences index with the rest.

2.2. Restrictions Due to COVID-19

To slow the spread of contagion in the first wave, the Mexican Government established “La Jornada Nacional de Sana Distancia” (JNSD) on March 23, 2020; see [Secretaría de Salud \(2020\)](#). The goal of the plan was to impose social distancing measures and reduce the spread of the virus by personal hygiene recommendations, guidelines for care of the elderly, suspension of activities deemed non-essential, and cancelling mass gathering events. The preventive measures ended on 30 May 2020, and were replaced by regional restrictions. Given the uniformity of the restrictions and thus the much simpler evaluation of compliance, we use JNSD in the first wave to evaluate their effects on mobility and air pollution. Figure 3 shows that JNSD produced a significant decrease in mobility in the MCMA.

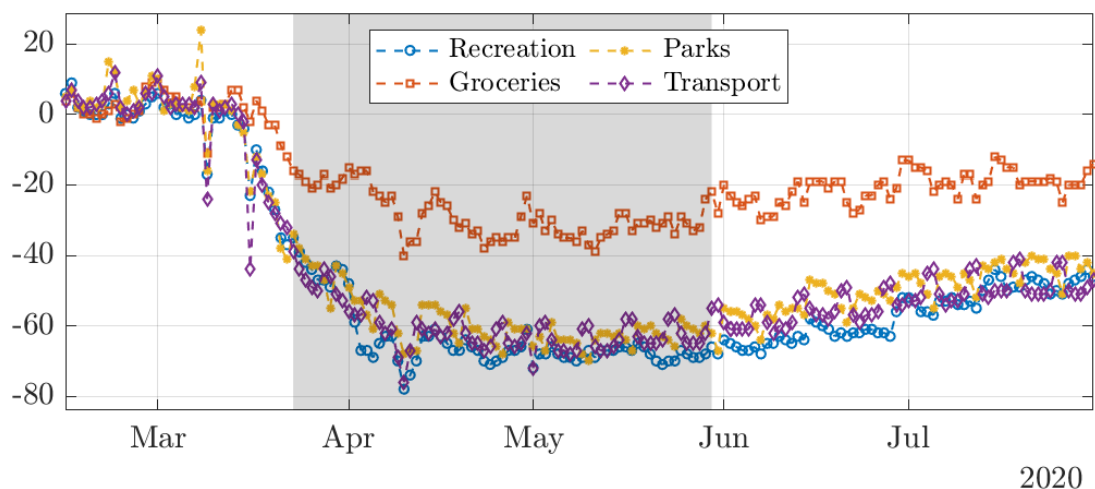


Figure 3. Google mobility indexes in the MCMA. JNSD is shown in the shaded area.

It has been shown that mobility reductions are correlated to a decrease in the number of COVID-19 cases ([Kraemer et al. 2020](#); [Nouvellet et al. 2021](#)). Thus, we would expect the reduction in mobility in the MCMA to affect the number of cases and deaths due to COVID-19.

Regarding air pollution, the evidence of the effect that restrictions due to the pandemic had on them is mixed. Significant reductions in air pollution are encountered in, among others, Brazil, India, Spain, and USA ([Baldasano 2020](#); [Berman and Ebusu 2020](#); [Nakada and Urban 2020](#); [Shehzad et al. 2020](#)). However, [Adams \(2020\)](#) finds that levels of PM 2.5 did not change in response to a region-wide state of emergency in Ontario, Canada. Figure 4 displays pollution series (PM2.5 and PM10) in the MCMA from July 2019 to July 2020 and reveals that the MCMA did not experience a significant reduction in air pollution during and after the COVID-19 lockdown, see [Vera-Valdés and Rodríguez-Caballero \(2021\)](#) for formal statistical tests. Thus, in contrast to other countries, the hypothesis of air pollution serving as a carrier for SARS-CoV-2 can be tested without endogenous decreases in the level of air pollution due to the restrictions.

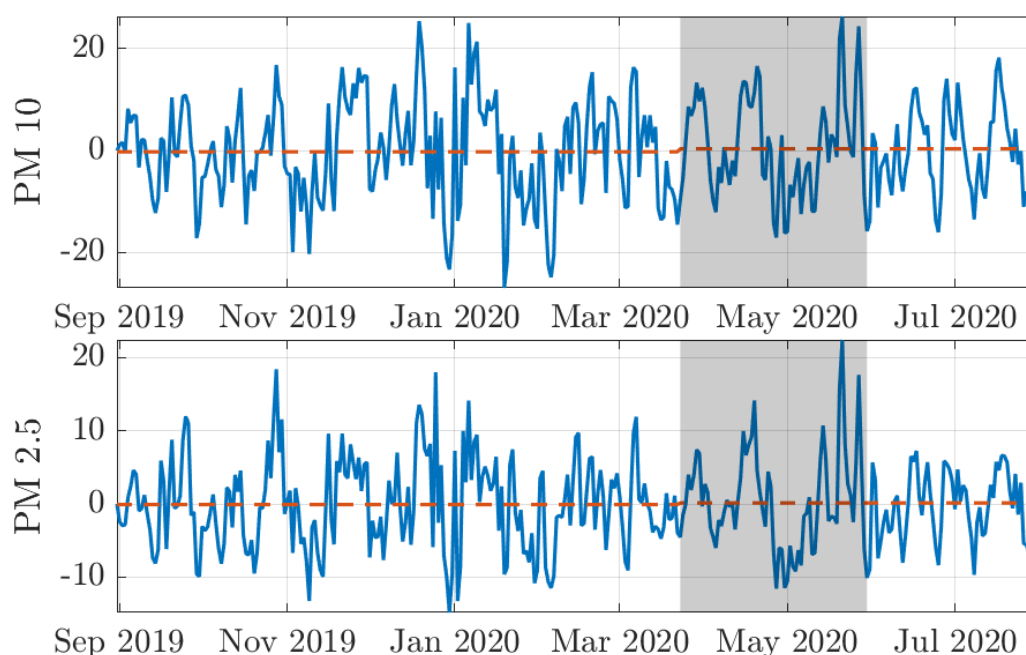


Figure 4. Air pollution indexes in the MCMA. The figure shows the actual levels (solid), and the fitted values to a test for change in level (dashed). JNSD is shown in the shaded area.

3. Econometric Methodology

Panel data models have been widely used in recent years as an alternative to handle the large number of time series recently found in modern empirical exercises. The main goal is to disentangle the complex phenomena due to the facility of exploiting the heterogeneity presented between cross-section units.

Parallel to the literature on dynamic factor modeling, unobservable common factors have been also used in the second-generation of panel data models, which assume that a factor structure drives the (strong) cross-dependence among units. Such models are called panel data with cross-sectional dependence. We employ such models to unravel the effect of mobility restrictions and contemporaneous air pollution exposure on the number of cases and deaths due to COVID-19. The applied literature frequently uses two popular approaches to estimate these factors.

A first approach is the Common Correlated Effects Mean Group (CCEMG) method of [Pesaran \(2006\)](#) that uses cross-sectional averages of the observable variables as good proxies for unobservable common factors. The second approach is the interactive fixed effects (IFEs) method proposed by [Bai \(2009\)](#). Instead of filtering unobserved common factors by a cross-sectional average of observed variables as in the CCEMG method, the IFE method estimates the common component together with the structural parameters of the panel model using Principal Component Analysis (PCA), which requires a prior knowledge of the number of factors.

Our interest in using this model is twofold: (i) controlling for time-invariant effects such as population density, average income level, etc.; and (ii) assessing the effect of controlling for the time-variant commonality between municipalities. The common factor allows us to control for variables like mobility restrictions affecting the entire MCMA, and avoid the simultaneity problem due to the nature of the factor structure, see [Bai and Ng \(2008\)](#).

To test if contemporaneous exposure to air pollutants is associated with SARS-CoV-2 spread, we consider the following model. Let the subindex (i, t) be the observation on the i -th municipality at time t for $i = 1, \dots, 21$; $t = 1, \dots, 137$; and consider the following linear panel data model with cross-sectional dependence

$$\begin{aligned}
 Y_{it} &= \alpha_i + \beta_{1,i}PM10_{i,t-k} + \beta_{2,i}PM25_{i,t-k} + e_{it}, \\
 e_{it} &= \lambda_i'F_t + \epsilon_{it},
 \end{aligned}
 \tag{1}$$

where Y_{it} is the number of cases or deaths as the case may be, $PM10$ and $PM25$ are air pollution measurements, the lag k controls for incubation time of the virus (with $k = 7, 14$ days), and α_i controls for all time-invariant confounding factors usually called as fixed effects. Remaining controls include health and economics variables that may affect the number of cases or deaths but that do not change in the period covered like population density, age distribution, healthcare expenditure, life expectancy, obesity levels, etc. Furthermore, e_{it} has a factor structure where λ_i is a $(r \times 1)$ vector of factor loadings; $F_t (r \times 1)$ is a vector of common factors so that $\lambda_i'F_t = \lambda_{i1}F_{1t} + \dots + \lambda_{ir}F_{rt}$; and ϵ_{it} are idiosyncratic errors. Finally, it is assumed that λ_i , F_t , and ϵ_{it} are all unobserved.

Estimation of the model is performed using three approaches; (i) the Mean Group (MG) estimator of Pesaran and Smith (1995), (ii) the CCEMG method of Pesaran (2006), and (iii) the Interactive Fixed Effects (IFE) method proposed by Bai (2009). These approaches allow us to assess the effect that the common factor has on the specification. MGE is based on the average of individual regressions and assumes that municipalities are independent of each other; thus, the common factor, F_t , is not considered.

Under Pesaran's approach, the main interest is to estimate the slope heterogeneous coefficients $\beta_{j,i}$ for $j = 1, 2$ which are computed by $\hat{\beta}_i = (\mathbf{X}_i' \overline{\mathbf{M}} \mathbf{X}_i)^{-1} \mathbf{X}_i' \overline{\mathbf{M}} \mathbf{y}_i$, where $\mathbf{X}_i = (\mathbf{x}_{i1}, \dots, \mathbf{x}_{iT})'$ are the explanatory variables; $\mathbf{y}_i = (y_{i1}, \dots, y_{iT})'$ the explained variable; and $\overline{\mathbf{M}} = \mathbf{I}_T - \overline{\mathbf{H}}(\overline{\mathbf{H}}' \overline{\mathbf{H}})^{-1} \overline{\mathbf{H}}'$ the projection matrix, with $\overline{\mathbf{H}} = (\mathbf{h}_1, \dots, \mathbf{h}_T)'$ a matrix of cross-sectional averages for the observables, and $(\overline{\mathbf{H}}' \overline{\mathbf{H}})^{-}$ denote the generalized inverse of $(\overline{\mathbf{H}}' \overline{\mathbf{H}})$. The CCEMG estimator for a particular pollutant is obtained by $\beta_{CCEMG} = \frac{1}{21} \sum_{i=1}^{21} \beta_i$.³ See Pesaran (2006) for technical details.

On the other hand, IFE estimation is based on a two-step procedure to capture the common factor and handle the commonality among municipalities. In the first step, IFE estimates the slope coefficients, while in the second step, the factor structure is extracted using Principal Component Analysis on residuals from the previous step.⁴ Then, the estimator for β is obtained by solving

$$\begin{aligned}
 \hat{\beta}_{PC} &= \left(\sum_{i=1}^N \mathbf{X}_i' \mathbf{M}_{F_{PC}} \mathbf{X}_i \right)^{-1} \sum_{i=1}^N \mathbf{X}_i' \mathbf{M}_{F_{PC}} \mathbf{y}_i, \quad \text{and} \\
 \frac{1}{NT} \sum_{i=1}^N (\mathbf{y}_i - \mathbf{X}_i \hat{\beta}_{PC}) (\mathbf{y}_i - \mathbf{X}_i \hat{\beta}_{PC})' \hat{\mathbf{F}}_{PC} &= \hat{\mathbf{F}}_{PC} \hat{\mathbf{V}}
 \end{aligned}$$

where $\mathbf{M}_{F_{PC}} = \mathbf{I}_T - \hat{\mathbf{F}}_{PC} (\hat{\mathbf{F}}_{PC}' \hat{\mathbf{F}}_{PC})^{-1} \hat{\mathbf{F}}_{PC}'$, with a $T \times r$ matrix $\hat{\mathbf{F}}_{PC}$ consists of the main r eigenvectors ($\times \sqrt{T}$) of the matrix $\frac{1}{NT} \sum_{i=1}^N (\mathbf{y}_i - \mathbf{X}_i \hat{\beta}_{PC}) (\mathbf{y}_i - \mathbf{X}_i \hat{\beta}_{PC})'$, while $\hat{\mathbf{V}}$ is the $r \times r$ diagonal matrix that has the r largest eigenvalues.

As mentioned before, the factor structure can absorb classical additive individual and time effects, nevertheless, as Bai (2009) points out, it is a good idea to model them explicitly to avoid inefficient estimators. Therefore, we consider a particular IFE model that includes the joint presence of additive and interactive effects as follows

$$Y_{it} = \mu + \alpha_i + \zeta_t + \beta_{1,i}PM10_{i,t-k} + \beta_{2,i}PM25_{i,t-k} + \lambda_i'F_t + \epsilon_{it},
 \tag{2}$$

where μ is a constant or grand mean, ζ_t is the time effect, and the remaining components are as before. The term interactive effect is used to indicate that the unobserved component, $\lambda_i'F_t$, enters the model multiplicatively, see Bai (2009) for technical details.

4. Testing for Stationarity and Cross-Sectional Dependence

The first step in our empirical analysis is to establish the statistical properties of our variables. On the one hand, to motivate the usefulness of our panel data models, we show that cross-sectional dependence has to be incorporated in the specification by the Exponent of Cross-Sectional Dependence of Bailey et al. (2016). Since such a test requires stationarity, we run first unit root tests. Additionally, we also need to guarantee stationarity for the estimation and inferences of the three approaches introduced in the previous section (MG, CCEMG, and IFE), although non-stationary extensions can be consulted in Kapetanios et al. (2011), Ergemen and Velasco (2017), and Rodríguez-Caballero (2021).

As natural in time-series analysis, a way to testing the unit root hypothesis is with standard ADF-family tests⁵. Nevertheless, it is well-known that single time-series test might not reject the null hypothesis of non-stationarity when we have a panel of time series. Therefore, we also employ two panel unit root tests; (i) the Fisher combination test (MW) developed by Maddala and Wu (1999), and (ii) the cross-sectionally augmented IPS (CIPS) test of Pesaran (2007). The first test belongs to the first-generation and ignores cross-section dependence in the data, whereas the second one allows for the presence of a single unobserved common factor with heterogeneous factor loadings and belongs to the called second-generation of panel unit-root tests. Pesaran (2007) exemplifies by simulations that tests that do not account for cross-sectional dependencies tend to over-reject the null due to considerable size distortion. Results are summarized in Table 1.

Table 1. Fisher combination (MW) and Cross-sectionally augmented IPS (CIPS) tests for panel unit roots.

	MW. Maddala and Wu (1999)				CIPS. Pesaran (2007)			
	15D		7D		15D		7D	
	Without Trend		With Trend		Without Trend		With Trend	
Death toll	50.778 ***	46.362 ***	41.466 ***	40.858 ***	−5.027 ***	−5.461 ***	−5.597 ***	−5.979 ***
Cases	64.173 ***	48.814 ***	130.05 ***	127.100 ***	−3.533 ***	−3.744 ***	−4.511 ***	−4.681 ***
PM10	44.345 ***	47.272 ***	57.327 ***	69.405 ***	−6.164 ***	−6.929 ***	−5.173 ***	−5.918 ***
PM2.5	41.298 ***	44.364 ***	36.233 ***	41.658 ***	−6.295 ***	−6.878 ***	−5.503 ***	−6.100 ***

Notes: This table reports the panel unit root test tests of the variables used in the study for the incubation period of 15 and 7 days. The null hypothesis in both methods is that panel series is $I(1)$. We set the lag order, $\hat{p} = [4(T/100)^{0.25}] = 4$ as in Pesaran et al. (2013). Models without and with trends are indicated in the respective columns. Asterisks (*, **, and ***) indicate significance at the 10%, 5% and 1% levels, respectively.

As seen in Table 1, the null hypothesis of unit root is strongly rejected in all cases regardless of whether the cross-sectional dependence is considered in the test or not. Although we have chosen $\hat{p} = [4(T/100)^{0.25}] = 4$ lags following Pesaran et al. (2013), we find same results irrespective of the lag order, $p < 4$, for all variables under investigation.⁶

With stationarity in hand, the next step is to confirm that cross-sectional dependence should be added in our panel data models. We run the Exponent of Cross-Sectional Dependence of Bailey et al. (2016) to measure the degree of dependence between municipalities across MCMA. Such a degree, denoted by α , can take any value in the range $[0, 1]$ and defines the type of dependence as follows: weak for $\alpha = 0$, semi-weak for $0 < \alpha < 0.5$, semi-strong for $0.5 < \alpha < 1$, and strong for $\alpha = 1$. The last two cases are consistent with the common factor literature, mainly if $\alpha = 1$. Table 2 shows results.⁷

As reported in Table 2, $\hat{\alpha}$ is estimated as approximately the unity for all variables, while the 95% confidence bands lie above 0.5. The findings so far show clearly the presence of strong cross-sectional dependence, particularly, we highlight that a factor structure can be assumed to reflect such dependence.

Table 2. Estimation of cross-sectional exponent and test of Bailey et al. (2016).

	$\hat{\alpha}$	Std. Err.	[95% Conf. Interval]	
			Inc. Period. 15 D	
Death toll	0.999	0.067	0.867	1.131
Cases	1.001	0.038	0.925	1.078
PM10	1.001	0.041	0.919	1.083
PM2.5	1.001	0.049	0.904	1.098
			Inc. Period. 7 D	
Death toll	1.001	0.071	0.860	1.140
Cases	1.001	0.046	0.910	1.093
PM10	1.002	0.047	0.909	1.094
PM2.5	1.002	0.076	0.851	1.151

Notes: This table reports the estimates of the exponent of cross-sectional dependence of variables used in the study for the incubation period of 15 and 7 days. We use two principle components for the calculation of (bias-adjusted) $\hat{\alpha}$.

5. Main Estimation Results

We present the main results on the effects of contemporaneous exposure to air pollution on the number of cases and deaths due to COVID-19 obtained using the estimators MG, CCEMG, and IFE, previously introduced. The main goal of this paper is, on the one hand, detecting whether the exposure to air pollution would increase the rhythm of contagion or death toll due to the virus SARS-COV2 in the sort-run, and, on the other hand, identifying whether an unobservable common factor is driving the rhythm of current pandemic between municipalities in the MCMA. While we focus on the IFE method, we also present the results obtained using alternative specifications.

Table 3 shows the estimation of the model specified in Equations (1) and (2). As previously discussed, findings reported in Table 2 indicated the presence of strong cross-sectional dependence. This is of great relevance because when one estimates a panel model, only this type of dependence may provoke serious inconsistencies. MG method ignored (semi-) strong dependence in the model, therefore, MG estimates might be inconsistent due to an omitted variable bias. In contrast, both the CCEMG and IFE methods added a factor structure in the specification to account for a strong cross-sectional dependence. In the IFE method, the number of common factors needs to be specified before estimating the model. We present results considering only one factor, but results did not differ when assuming two.⁸

Results from Table 3 reveal that contemporary air pollution exposure was only statistically significant for the number of cases and deaths, disregarding the incubation period, only when the specification neglected a strong cross-sectional dependence (see column MG). Overall, the use of the CCEMG and IFE methods confirmed the main findings and provides some further insights. That is, there was no evidence that air pollution served as a carrier for SARS-CoV-2 in the sort-run once we added a factor structure⁹.

Our findings may generate a debate because there is much evidence that argues for a positive correlation between (long-term) air pollution exposure and the death toll due to COVID-19, see e.g., Yao et al. (2020), Gupta et al. (2020) and Bianconi et al. (2020). However, our results are in line with those of Rodriguez-Villamizar et al. (2020) who also find no evidence of an association between long-term exposure to PM 2.5 and COVID-19 mortality either rate in Colombia, another Latin American country. A new open question could be related to unraveling whether the relationship between exposure to air pollution and the number of deaths from COVID-19 varies according to the economic regions or the social realities of the countries.

Table 3. Estimation of specification (1) and (2) considering several incubation periods.

Dep. Variable Incubation Model	Daily Death Toll					
	MG	14 Days CCEMG	IFE	MG	7 Days CCEMG	IFE
PM10	−0.149 *** (0.031)	0.017 (0.030)	−0.044 (0.024)	−0.190 *** (0.045)	−0.001 (0.035)	−0.021 (0.022)
PM2.5	0.240 *** (0.051)	−0.016 (0.029)	0.063 (0.039)	0.0261 *** (0.071)	0.054 (0.034)	0.031 (0.024)
constant	4.916 *** (1.316)	−0.090 (0.811)	4.840 *** (0.070)	5.745 *** (1.493)	0.152 (0.555)	3.600 *** (0.051)
R^2	0.547	0.803	0.847	0.538	0.800	0.925
$ \bar{\rho} $	0.239	0.083	0.064	0.636	0.079	−0.061
CIPS	−4.802 ***	−5.341 ***	−5.451 ***	−3.503 ***	−4.154 ***	−4.554 ***
J_{KSS}			55.36 ***			62.29 ***
Dep. Variable Incubation Model	Daily number of cases					
	MG	14 days CCEMG	IFE	MG	7 days CCEMG	IFE
PM10	−1.139 *** (0.216)	−0.034 (0.198)	−0.019 (0.107)	−1.287 *** (0.295)	0.027 (0.101)	−0.034 (0.103)
PM2.5	1.318 *** (0.231)	0.042 (0.242)	−0.103 (0.169)	1.350 *** (2.212)	0.082 (0.216)	−0.045 (0.163)
constant	51.359 *** (11.604)	−0.041 (1.330)	40.100 *** (0.309)	53.137 *** (11.767)	1.402 (1.539)	37.300 *** (0.291)
R^2	0.583	0.931	0.940	0.554	0.933	0.943
$ \bar{\rho} $	0.250	0.066	0.066	0.649	0.061	0.060
CIPS	−4.829 ***	−5.492 ***	−5.674 ***	−3.664 ***	−3.859 ***	−4.149 ***
J_{KSS}			114.11 ***			139.81 ***

Notes: Robust Newey-West standard errors in parentheses (robust against any type of intragroup heteroskedasticity and serial correlation) for all cases. R^2 is the mean of the cross-sectional individual R^2 weighted by the overall error variance. $|\bar{\rho}|$ is the absolute average correlation coefficient. The null in the CIPS test is not stationarity, see Pesaran (2007). The IFE model assumes joint presence of additive and interactive effects, bias corrected coefficients are reported in the table, see Bai (2009). The null in the J_{KSS} test is no factor structure is required in the model. Asterisks (*, **, and ***) indicate significance at the 10%, 5% and 1% levels, respectively.

A further inspection on Table 3 provide some relevant remarks. First, the absolute average correlation coefficient, $|\bar{\rho}|$, indicates that the cross-correlation in the panel decreases when incorporating a factor structure. Second, the CIPS test of Pesaran (2007) shows that residuals are always stationary. Third, the specification test proposed by Kneip et al. (2012), J_{KSS} , shows that a factor structure is always required in the IFE model over classical additive (individual and time) effects model to describe the data.

To shed light on the nature of the common factor, Table 4 and Figure 5 show that F_t is highly correlated to the Google mobility indexes in the MCMA reported in Figure 3. Therefore, the dynamics of COVID-19 spread is mainly due to human-to-human transmission rather than air pollution-to-human transmission.

Our findings suggest that governments should point to strong and timely restrictions to mobility measures to prevent and contain the spread of COVID-19 in the short-run instead of focusing efforts to control air pollution.

To the best of our knowledge, this paper is the first to analyze the joint effect that reduced mobility and air pollution have on the rhythm of contagion and the death toll due to the pandemic of COVID 19. Our results showed that mobility restrictions had a significant effect on reducing the number of cases and deaths due to COVID-19 irrespective

of the air pollution levels in the short-term. Thus, the carrier hypothesis was not supported for SARS-CoV2.

Table 4. Common factor correlations with mobility indexes considering additional incubation periods.

Mobility Index	Daily Death Toll		Daily Number of Cases	
	14 Days	7 Days	14 Days	7 Days
Recreation	0.730	0.658	0.447	0.408
Groceries	0.691	0.662	0.488	0.355
Parks	0.751	0.663	0.426	0.296
Transport	0.675	0.588	0.490	0.558

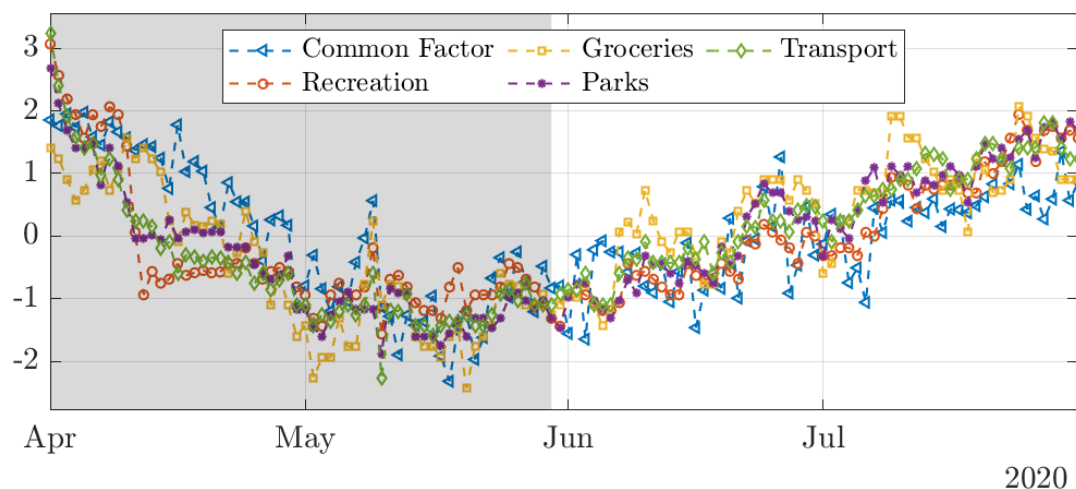


Figure 5. Common factor and Google mobility indexes (scaled) for the specification considering the number of deaths due to COVID-19 and an incubation period of 14 days. JNSD is shown in the shaded area.

To accompany the analysis of the common component, Figure 6 displays the weights of factor loadings. Note that the signs are all negative. These loadings show that the municipalities with the highest number of deaths have the highest (negative) magnitudes. These loadings indicate the impact of reducing mobility on the death toll during JNSD. Thus, the policy of mobility restrictions during the JNSD helped to decrease the mortality due to COVID-19. Our findings indicate that these decrements were considerably more relevant in municipalities where people's flux is high, such as in Iztapalapa and Ecatepec; two regions in the MCMA with the highest rate of population density as detailed in Figure 1.

The analysis of the common factor and loadings revealed what occurred in Mexico in the first months of the current COVID 19 situation. The federal government declared the third phase on 21 April 2020, as a consequence of the exponential increase in COVID-19 cases. The contingency plan to fight against the virus at this stage consisted of an unforced lockdown, contrary to other countries in the world. Although all public events were officially canceled, and non-essential activities were suspended. As Figure A1 shows, the daily-life dynamic in the MCMA before the pandemic showed an important flux of people moving from the periphery of the city (Iztapalapa or Ecatepec) to the business and financial districts (Benito Juarez or Cuajimalpa), particularly on weekdays. In 2020, thanks to the aforementioned third phase, the people of the most populated municipalities found conditions to stop moving to the financial zones. However, when the JNSD officially ended (on 30 May), some restrictions were relaxed. Consequently, the flux of people increased again, which is clearly displayed in Figure 5. This analysis of the public mobility in the MCMA could warn people to try to decrease their activities during the worst time of a difficult health situation. Of course, if economic conditions allow it. The common factor also captures this apparent change in the slope immediately after the shaded area.

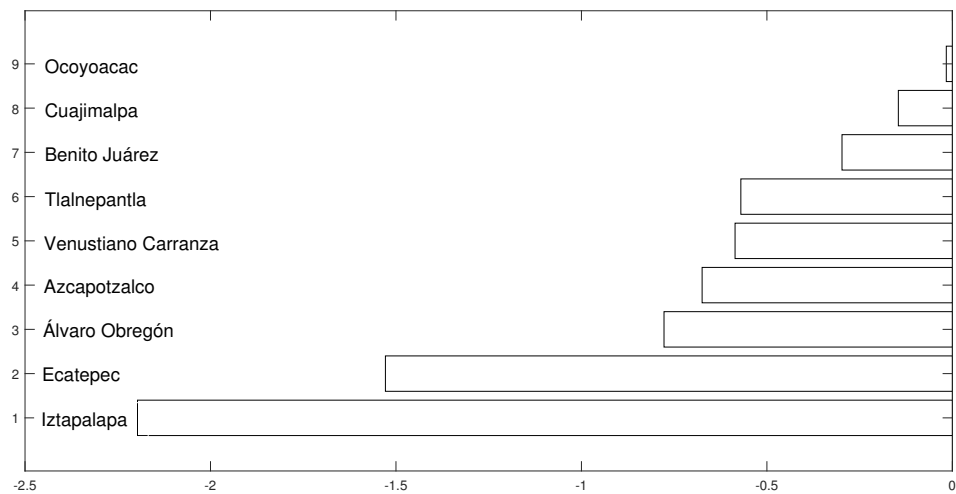


Figure 6. Factor loadings.

6. Future Extensions and Limitations

6.1. Future Extensions

A possible future extension may point to analyzing the behavior of factor loadings over time due to the constant change in social dynamics, which is not assumed in the panel data model previously considered. Here, we provided some preliminary ideas and results. We iterate the procedure one more time and estimate the factor model with time-varying loadings recently proposed by Cataño et al. (2021). The methodology consists of two stages. First, the common factors are estimated by PCA, and in the second stage, the time-varying loadings are estimated by an iterative procedure of generalized least squares and wavelet functions. The advantage of their approach relies on smooth, and progressive variations (smooth deterministic or seasonal trends) that are assumed to drive the behavior of the factor loadings. Figure 7 displays results.

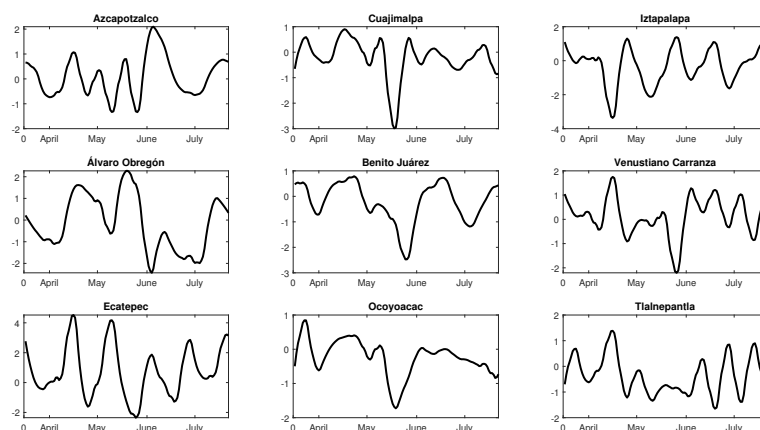


Figure 7. Estimation of the time-varying loadings of model in Equation (2) by Cataño et al. (2021).

At first glance, time-varying loadings indicate a smooth variation with seasonal signals. Cuajimalpa, Benito Juárez, Ocoyoacac share similar behaviors showing local maximums and minimums on similar dates, while the remaining share another dynamic with slightly more seasonal changes along time. Particularly, in Cuajimalpa and Benito Juárez, we can observe a clear decrease in loadings during the JNSD, which may be related to daily life in both zones. Then, when the third phase started, these municipalities experienced a

relevant decrease in people's flux, helping both zones reduce the rhythm of contagion and, consequently, the death toll.

6.2. Limitations

There are some limitations in the present study that can be improved in future analyses. Among others, two of them are:

- Our data only include the first wave of the pandemic in the MCMA. However, a year after the first wave, as many other countries in the world, Mexico has faced second and third waves. Unfortunately, the public RAMA database has been moved to another repository, and it could not be consulted by the time this paper was written.
- Models (1) and (2) do not cover the case where the panel includes a lagged dependent variable limiting a deeper dynamic analysis. In this respect, possible improvements can be considering models proposed by [Chudik and Pesaran \(2015\)](#), and [Moon and Weidner \(2017\)](#).

7. Conclusions

This paper analyzes the relation between air pollution exposure and the number of cases and deaths due to COVID-19 in the MCMA. We test if air pollution serves as a carrier for SARS-CoV-2. To the best of our knowledge, this paper is the first to disentangle the synergistic effect of reduced mobility and air pollution on the virus spread.

Our results show that contemporaneous exposure to air pollutants is only statistically significant to explain the number of cases and deaths when the commonality between municipalities is neglected. Furthermore, the common factor is shown to be highly correlated to mobility. Consequently, we argue that in the short-term, the dynamics of COVID-19 spread is mainly due to human-to-human rather than air pollution-to-human transmission. These results are particularly revealing given the fact that the MCMA did not experience a decrease in air pollutants during the first COVID-19 lockdown.

Our findings' policy implications are related to the higher death toll scenarios provoked by the current pandemic in areas marked by high population density and a dynamic lifestyle. Our results suggest that governments should implement policies to reduce mobility to mitigate health risks due to the pandemic. Since mobility constraints are the main driver behind the pace of contagion, it can help in reducing the number of deaths due to COVID-19 in the short-term.

To conclude, we offer a warning to policymakers for the short term. This pandemic has shown that the worst scenarios are emerging in areas commonly marked by high population density and with a highly dynamic lifestyle. Then, to help control and not only mitigate the exceptional rate of contagion and death toll, we highlight the necessity of implementing policies to reduce mobility, which is the main driver behind the pace of contagion and it can help in reducing the number of deaths due to COVID-19.

Author Contributions: The two authors of the paper have contributed equally in conceptualization, methodology, formal analysis, validation, data curation, writing, and editing. The authors are responsible for all remaining errors. All authors have read and agreed to the published version of the manuscript.

Funding: This research did not receive any specific grant from funding agencies in the public, commercial, or not-for-profit sectors.

Institutional Review Board Statement: Not applicable.

Informed Consent Statement: Not applicable.

Data Availability Statement: The data that support the findings of this study are publicly available at datos.cdmx.gob.mx (accessed on 20 September 2020) and google.com/covid19/mobility/ (accessed on 16 January 2021).

Acknowledgments: We are indebted to Alejandro López-Feldman for his invaluable comments in a previous version of the paper, and Duván Humberto Cataño for the technical assistance in the short extension. We are also thankful to the associate editor and two anonymous referees for a speedy and high-quality evaluation procedure. The first author thanks the participants at the XXXIV conference of the Mexican Statistical Association. Any remaining errors are ours. This research was supported by Asociación Mexicana de Cultura, A.C.

Conflicts of Interest: The authors declare no conflict of interest.

Appendix A

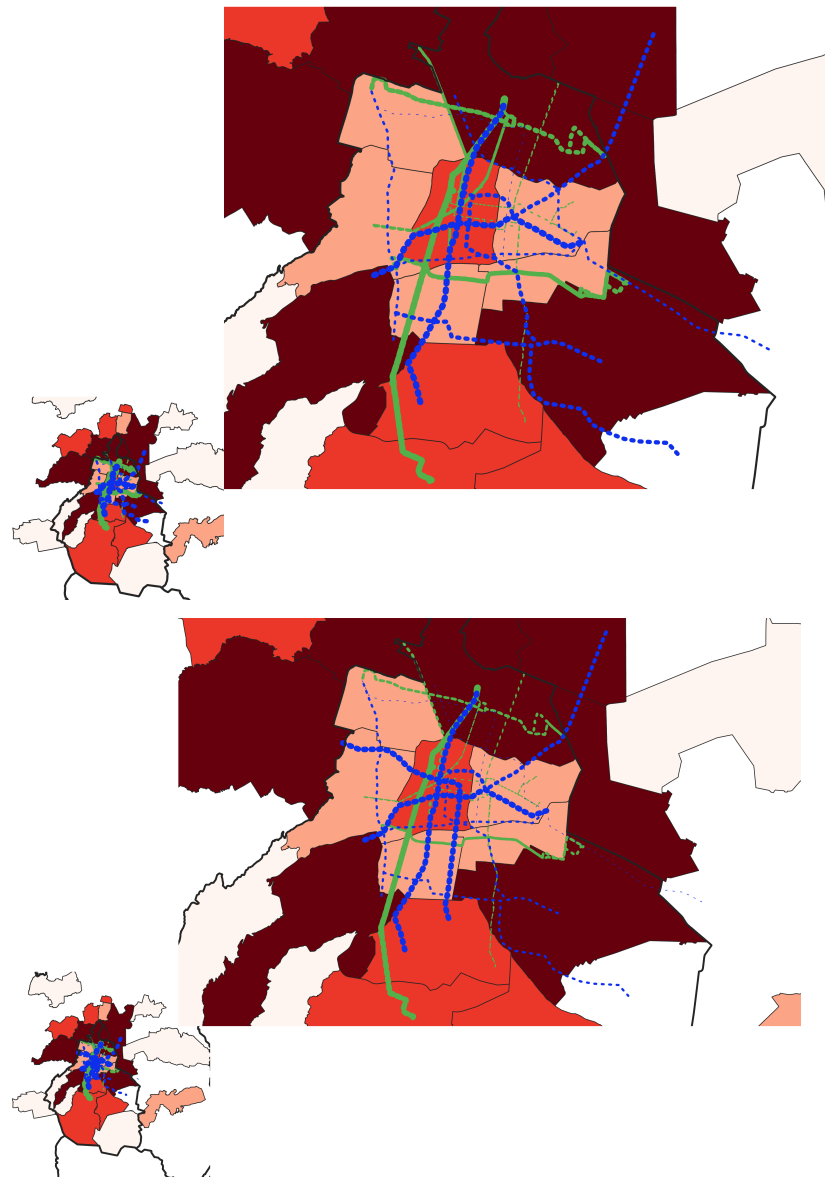


Figure A1. Plot of the annual average of public transport mobility on weekdays (**top**) and on weekend (**bottom**) in the MCMA in 2019. Subways and BRT lines are indicated in blue and green colors, respectively. The wider the color lines, the more public mobility. Source: Compiled by authors using data from INEGI.

Notes

- ¹ The link is tomtom.com/en_gb/traffic-index/ranking/ (accessed on 1 November 2020).
- ² Available online at datos.cdmx.gob.mx (accessed on 20 September 2020).

- 3 Mulcollinearity might easily occur in a model in which cross-sectional dependence is approximated by cross-sectional averages such as in the Pesaran's approach. Some software codes check automatically for collinearity in data and chose an efficient algorithm to invert the data matrices. An usual method is by the generalized inverse as in Pesaran (2006).
- 4 Another difference between both approaches is the assumption regarding slope parameters. The MGE method assumes heterogeneous parameters, while IFE works with homogeneous slopes, i.e., $\alpha_i = \alpha$, $\beta_{1,i} = \beta_1$, $\beta_{2,i} = \beta_2$, and $\beta_{3,i} = \beta_3$ for all i .
- 5 The analysis reports that all variables involved are stationary. Results are not reported here for the sake of brevity, but available upon request.
- 6 Pesaran's CIPS test performances well in small-sample in the presence of a single unobserved common factor, however, if the number of common factors is higher, the test exhibits size distortions. In this respect, Pesaran et al. (2013) propose an extension to cover a multi-factor error structure. We employ the CIPS and CSB tests proposed for $r = 1, 2, 3$ number of factors and we find the same conclusions. Tables are available upon request.
- 7 We employ the stata routine 'xtcse2' provided by Ditzen (2019).
- 8 The second common factor is correlated to climatological variables such as temperature and wind, which is in line with the results of Coccia (2021). For reasons of space, the results are not shown here but they are available upon request.
- 9 The plots for actual and fitted series, as well as that of the residual are available upon request

References

- Adams, Matthew D. 2020. Air pollution in Ontario, Canada during the COVID-19 State of Emergency. *Science of The Total Environment* 742: 140516. [CrossRef]
- Bai, Jushan, and Serena Ng. 2008. *Large Dimensional Factor Analysis*. Norwell: Now Publishers Inc.
- Bai, Jushan. 2009. Panel data models with interactive fixed effects. *Econometrica* 77: 1229–79.
- Bailey, Natalia, George Kapetanios, and M. Hashem Pesaran. 2016. Exponent of cross-sectional dependence: Estimation and inference. *Journal of Applied Econometrics* 31: 929–60. [CrossRef]
- Baldasano, José M. 2020. COVID-19 lockdown effects on air quality by NO₂ in the cities of Barcelona and Madrid (Spain). *Science of The Total Environment* 741: 140353. [CrossRef] [PubMed]
- Berman, Jesse D., and Keita Ebisu. 2020. Changes in U.S. air pollution during the COVID-19 pandemic. *Science of The Total Environment* 739: 139864. [CrossRef]
- Bianconi, Vanessa, Paola Bronzo, Maciej Banach, Amirhossein Sahebkar, Massimo Mannarino, and Matteo Pirro. 2020. Particulate matter pollution and the COVID-19 outbreak: Results from Italian regions and provinces. *Archives of Medical Science* 16: 985–92. [CrossRef] [PubMed]
- Borisova, Tatiana, and Serhiy Komisarenko. 2020. Air pollution particulate matter as a potential carrier of SARS-CoV-2 to the nervous system and/or neurological symptom enhancer: Arguments in favor. *Environmental Science and Pollution Research*. [CrossRef]
- Cataño, Duván Humberto, C. Vladimir Rodríguez-Caballero, Daniel Peña, and Chang Chiann. 2021. Wavelet estimation for factor models with time-varying loadings. *International Journal of Wavelets, Multiresolution and Information Processing*. [CrossRef]
- Chudasama, Yogini V., Clare L. Gillies, Karen Appiah, Francesco Zaccardi, Cameron Razieh, Melanie J. Davies, Thomas Yates, and Kamlesh Khunti. 2020. Multimorbidity and SARS-CoV-2 infection in UK Biobank. *Diabetes & Metabolic Syndrome* 14: 775–76. [CrossRef].
- Chudik, Alexander, and M. Hashem Pesaran. 2015. Common correlated effects estimation of heterogeneous dynamic panel data models with weakly exogenous regressors. *Journal of Econometrics* 188: 393–420. [CrossRef]
- Coccia, Mario. 2021. The effects of atmospheric stability with low wind speed and of air pollution on the accelerated transmission dynamics of COVID-19. *International Journal of Environmental Studies* 78: 1–27. [CrossRef]
- Comunian, Silvia, Dario Dongo, Chiara Milani, and Paola Palestini. 2020. Air pollution and covid-19: The role of particulate matter in the spread and increase of covid-19's morbidity and mortality. *International Journal of Environmental Research and Public Health* 17: 4487. [CrossRef] [PubMed]
- Coticini, Edoardo, Bruno Frediani, and Dario Caro. 2020. Can atmospheric pollution be considered a co-factor in extremely high level of SARS-CoV-2 lethality in Northern Italy? *Environmental Pollution* 261: 114465. [CrossRef] [PubMed]
- Ditzen, Jan. 2021. Xtcse2: Stata Module to Estimate the Exponent of Cross-Sectional Dependence in Large Panels. Available online: <https://EconPapers.repec.org/RePEc:boc:bocode:s458670> (accessed on 20 September 2020).
- Ergemen, Yunus, and Carlos Velasco. 2017. Estimation of fractionally integrated panels with fixed effects and cross-section dependence. *Journal of Econometrics* 196: 248–58. [CrossRef]
- Farias Costa, Fernanda, Wilian Reis Rosário, Ana Cláudia Ribeiro Farias, Ramon Guimaraes de Souza, and Roberta Sabrina Duarte Gondim. 2020. Metabolic syndrome and COVID-19: An update on the associated comorbidities and proposed therapies. *Diabetes & Metabolic Syndrome: Clinical Research & Reviews* 14: 809–14. [CrossRef]
- Frontera, Antonio, Lorenzo Cianfanelli, Konstantinos Vlachos, Giovanni Landoni, and George Cremona. 2020. Severe air pollution links to higher mortality in COVID-19 patients: The "double-hit" hypothesis. *Journal of Infection* 81: 255–59. [CrossRef] [PubMed]
- Google. 2020. COVID-19 Community Mobility Reports. Available online: <https://www.google.com/covid19/mobility/> (accessed on 16 January 2021).

- Groulx, Nicolas, Bruce Urch, Caroline Duchaine, Samira Mubareka, and James A. Scott. 2018. The Pollution Particulate Concentrator (PoPCon): A platform to investigate the effects of particulate air pollutants on viral infectivity. *Science of the Total Environment* 628–629: 1101–7. [CrossRef]
- Guerra, Erick. 2015. The geography of car ownership in Mexico City: A joint model of households' residential location and car ownership decisions. *Journal of Transport Geography* 43: 171–80. [CrossRef]
- Gupta, Ankit, Hemant Bherwani, Sneha Gautam, Saima Anjum, Kavya Musugu, Narendra Kumar, Avneesh Anshul, and Rakesh Kumar. 2020. Air pollution aggravating COVID-19 lethality? Exploration in Asian cities using statistical models. *Environment, Development and Sustainability*. [CrossRef] [PubMed]
- Instituto Federal de Telecomunicaciones. 2020. Evolución de la Adopción y el uso de las TIC en México 2015–2019. Available online: http://www.ift.org.mx/sites/default/files/contenidogeneral/estadisticas/evoluciondelastic2015-2019_0.pdf (accessed on 16 January 2021).
- Kapetanios, George, M. Hashem Pesaran, and Takashi Yamagata. 2011. Panels with non-stationary multifactor error structures. *Journal of Econometrics* 160: 326–48. [CrossRef]
- Kneip, Alois, Robin C. Sickles, and Wonho Song. 2012. A new panel data treatment for heterogeneity in time trends. *Econometric Theory* 28: 590–628. [CrossRef]
- Kraemer, Moritz U. G., Chia-Hung Yang, Bernardo Gutierrez, Chieh-Hsi Wu, Brennan Klein, David M. Pigott, Louis du Plessis, Nuno R. Faria, Ruoran Li, William P. Hanage, and et al. 2020. The effect of human mobility and control measures on the COVID-19 epidemic in China. *Science* 368: 493–97. [CrossRef]
- López-Feldman, Alejandro, David Heres, and Fernanda Marquez-Padilla. 2021. Air pollution exposure and COVID-19: A look at mortality in Mexico City using individual-level data. *Science of the Total Environment* 756: 143929. [CrossRef] [PubMed]
- Maddala, Gangadharrao S., and Shaowen Wu. 1999. A comparative study of unit root tests with panel data and a new simple test. *Oxford Bulletin of Economics and Statistics* 61: 631–52. [CrossRef]
- Marquès, Montse, Joaquim Rovira, Martí Nadal, and José L. Domingo. 2021. Effects of air pollution on the potential transmission and mortality of COVID-19: A preliminary case-study in Tarragona Province (Catalonia, Spain). *Environmental Research* 192: 110315. [CrossRef] [PubMed]
- Moffet, Ryan C., Yury Desyaterik, Rebecca J. Hopkins, Alexei V. Tivanski, Mary K. Gilles, Yu Wang, Vaithiyalingam Shutthanandan, Luisa T. Molina, Rodrigo Gonzalez Abraham, Kirsten S. Johnson, and et al. 2008. Characterization of aerosols containing Zn, Pb, and Cl from an industrial region of Mexico City. *Environmental Science & Technology* 42: 7091–97.
- Molina, Luisa, and Mario J. Molina. 2002. *Air Quality in the Mexico Megacity: An Integrated Assessment*. Berlin: Springer Science & Business Media, vol. 2.
- Moon, Hyungsik Roger, and Martin Weidner. 2017. Dynamic linear panel regression models with interactive fixed effects. *Econometric Theory* 33: 158–95. [CrossRef]
- Nakada, Liane Yuri Kondo, and Rodrigo Custodio Urban. 2020. COVID-19 pandemic: Impacts on the air quality during the partial lockdown in São Paulo state, Brazil. *Science of The Total Environment* 730: 139087. [CrossRef] [PubMed]
- Nouvellet, Pierre, Sangeeta Bhatia, Anne Cori, Kylie E. C. Ainslie, Kylie Baguelin, Samir Bhatt, Adhiratha Boonyasiri, Nicholas F. Brazeau, Lorenzo Cattarino, Laura V. Cooper, and et al. 2021. Reduction in mobility and COVID-19 transmission. *Nature Communications* 1–9. [CrossRef]
- Pesaran, M. Hashem, and Ron Smith. 1995. Estimating long-run relationships from dynamic heterogeneous panels. *Journal of Econometrics* 68: 79–113. [CrossRef]
- Pesaran, M. Hashem, L. Vanessa Smith, and Takashi Yamagata. 2013. Panel unit root tests in the presence of a multifactor error structure. *Journal of Econometrics* 175: 94–115. [CrossRef]
- Pesaran, M. Hashem. 2006. Estimation and inference in large heterogeneous panels with a multifactor error structure. *Econometrica* 74: 967–1012. [CrossRef]
- Pesaran, M. Hashem. 2007. A simple panel unit root test in the presence of cross-section dependence. *Journal of Applied Econometrics* 22: 265–312. [CrossRef]
- Rodríguez-Caballero, C. Vladimir, and J. Eduardo Vera-Valdés. 2020. Long-lasting economic effects of pandemics: Evidence on growth and unemployment. *Econometrics* 8: 37. [CrossRef]
- Rodríguez-Caballero, C. Vladimir. 2021. Energy consumption and GDP: A panel data analysis with multi-level cross-sectional dependence. *Econometrics and Statistics*. [CrossRef]
- Rodríguez-Villamizar, Laura A., Luis Carlos Belalcázar-Ceron, Julián Alfredo Fernández-Niño, Diana Marcela Marín-Pineda, Oscar Alberto Rojas-Sánchez, Lizbeth Alexandra Acuña-Merchán, Nathaly Ramírez-García, Sonia Cecilia Mangones-Matos, Jorge Mario Vargas-González, Julián Herrera-Torres, and et al. 2020. Air pollution, sociodemographic and health conditions effects on COVID-19 mortality in Colombia: An ecological study. *Science of the Total Environment*. [CrossRef]
- Secretaría de Salud. 2020. Jornada Nacional de Sana Distancia. Available online: https://www.gob.mx/cms/uploads/attachment/file/541687/Jornada_Nacional_de_Sana_Distancia.pdf (accessed on 20 September 2020).
- Setti, Leonardo, Fabrizio Passarini, Gianluigi De Gennaro, Pierluigi Barbieri, Maria Grazia Perrone, Massimo Borelli, Jolanda Palmisani, Alessia Di Gilio, Prisco Piscitelli, and Alessandro Miani. 2020. Airborne transmission route of COVID-19: Why 2 meters/6 feet of inter-personal distance could not be enough. *International Journal of Environmental Research and Public Health* 17: 2932. [CrossRef]

- Shehzad, Khurram, Muddassar Sarfraz, and Syed Ghulam Meran Shah. 2020. The impact of COVID-19 as a necessary evil on air pollution in India during the lockdown. *Environmental Pollution* 266: 115080. [CrossRef]
- Son, Ji-Young, Kelvin C. Fong, Seulkee Heo, Honghyok Kim, Chris C. Lim, and Michelle L. Bell. 2020. Reductions in mortality resulting from reduced air pollution levels due to COVID-19 mitigation measures. *Science of the Total Environment* 744: 141012. [CrossRef] [PubMed]
- Travaglio, Marco, Yizhou Yu, Rebeka Popovic, Liza Selley, Nuno Santos Leal, and Luis Miguel Martins. 2021. Links between air pollution and covid-19 in england. *Environmental Pollution* 268: 115859. [CrossRef]
- Vera-Valdés, J. Eduardo, and Rodríguez-Caballero, C. Vladimir. 2021. Air Pollution and Mobility in the Mexico City Metropolitan Area in Times of COVID-19. *Atmósfera*. Available online: <https://www.revistascca.unam.mx/atm/index.php/atm/article/view/53052> (accessed on 20 September 2020).
- Vera-Valdés, J. Eduardo. 2021. The political risk factors of COVID-19. *International Review of Applied Economics* 35: 269–287. [CrossRef]
- Westerlund, Joakim, and Jean-Pierre Urbain. 2015. Cross-sectional averages versus principal components. *Journal of Econometrics* 185: 372–77. [CrossRef]
- Yang, Jing, Ya Zheng, Xi Gou, Ke Pu, Zhaofeng Chen, Qinghong Guo, Rui Ji, Haojia Wang, Yuping Wang, and Yongning Zhou. 2020. Prevalence of comorbidities and its effects in patients infected with SARS-CoV-2: A systematic review and meta-analysis. *International Journal of Infectious Diseases* 94: 91–95. [CrossRef] [PubMed]
- Yao, Ye, Jinhua Pan, Weidong Wang, Zhixi Liu, Haidong Kan, Yang Qiu, Xia Meng, and Weibing Wang. 2020. Association of particulate matter pollution and case fatality rate of COVID-19 in 49 Chinese cities. *Science of The Total Environment* 741: 140396. [CrossRef] [PubMed]